

## USE OF UAV IMAGERY FOR EELGRASS MAPPING IN ATLANTIC CANADA

L. Aarts<sup>1</sup>, A. LaRocque<sup>2,\*</sup>, B. Leblon<sup>2,\*</sup>, A. Douglas<sup>3</sup>

<sup>1</sup> Faculty of Forestry and Environmental Management, University of New Brunswick, Fredericton (NB), Canada  
- aarts.lauren@gmail.com

<sup>2</sup> Faculty of Forestry and Environmental Management, University of New Brunswick, Fredericton (NB), Canada  
- (larocque, bleblon)@unb.ca

<sup>3</sup> Southern Gulf of St. Lawrence Coalition on Sustainability, Stratford (PEI), Canada - Coalition.sgsi@gmail.com

### Commission I, ICWG I/II

**KEY WORDS:** Eelgrass mapping, Atlantic Canada, UAV, Drone, RGB imagery

### ABSTRACT:

Eelgrass beds are critical in coastal ecosystems and can be useful as a measure of nearshore ecosystem health. Population declines have been seen around the world, including in Atlantic Canada. Restoration has the potential to aid the eelgrass population. Traditionally, field-level protocols would be used to monitor restoration; however, using unmanned aerial vehicles (UAVs) would be faster, more cost-efficient, and produce images with higher spatial resolution. This project used RGB UAV imagery and data acquired over five sites with eelgrass beds in the northern part of the Shediac Bay (New Brunswick, Canada). The images were mosaicked using Pix4Dmapper and PCI Geomatica. Each RGB mosaic was tested for the separability of four different classes (eelgrass bed, deep water channels, sand floor, and mud floor), and training areas were created for each class. The Maximum-likelihood classifier was then applied to each mosaic for creating a map of the five sites. With an average and overall accuracy higher than 98% and a Kappa coefficient higher than 0.97, the Pix4D RGB mosaic was superior to the PCI Geomatica RGB mosaic with an average accuracy of 89%, an overall accuracy of 87%, and a Kappa coefficient of 0.83. This study indicates that mapping eelgrass beds with UAV RGB imagery is possible, but that the mosaicking step is critical. However, some factors need to be considered for creating a better map, such as acquiring the images during overcast conditions to reduce the difference in sun illumination, and the effects of glint or cloud shadow on the images.

## 1. INTRODUCTION

Eelgrass beds are critical in coastal ecosystems as they provide vital ecological functions, including stabilizing sediment, providing fish habitat, influencing current dynamics, and contributing significant amounts of biomass to food webs (Heck et al., 1995). Eelgrass has the potential to serve as a sentinel of coastal environmental change associated with both natural and anthropogenic disturbances (Biber et al., 2004) and has proven useful as a measure of nearshore ecosystem health. While populations are stable under pristine conditions (Ward et al., 1997), eelgrasses around the world are declining at an annual rate of 7% of existing communities as a result of various types of disturbances in coastal and estuarine environments (Short, Wyllie-Echeverria, 1996). Declines in the eelgrass population have also been observed in Canada (Morris et al., 2011).

Restoration in areas with suitable habitat is a useful option to mitigate eelgrass decline and has the potential to re-establish the many essential ecosystem services eelgrass beds provide. Restoration success can be assessed using field-level protocols (Short et al., 2006), but they are time-consuming and labour-intensive. A flexible and cost-effective approach is to use an unmanned aerial vehicle (UAV) images. After its development for military applications, UAV has become a popular tool for civil applications (Peasgood, Valentin, 2015). This new technology is mobile, fast, adaptable, and easy to use. UAVs can also operate at much lower altitudes, which leads to images with higher spatial resolution than the ones acquired from aircraft and

spacecraft platforms (Pajares, 2015). So far, there have been only a few studies using UAV images for mapping eelgrass beds in tropical/Mediterranean and temperate environments using mostly RGB cameras (Ventura et al., 2018; Konar, Iken, 2017). While UAV technology can be advantageous, it has the drawback to require image mosaicking given the small footprint of UAV imagery.

The goal of this study is to compare the effect of two mosaicking packages (Pix4Dmapper and PCI Geomatica) on the classification accuracy obtained by applying a Maximum Likelihood classifier to RGB UAV imagery acquired over five eelgrass bed restoration sites, which are located inside a sheltered bay of Atlantic Canada.

## 2. MATERIAL AND METHODS

### 2.1 Materials

**2.1.1 Study area:** The experiment was conducted on five eelgrass sites located in the northern part of the Shediac Bay, New Brunswick, Canada (Latitude: 46° 16' 30" N; Longitude: 64° 34' 10" W), specifically at the mouth of the Shediac River, near Shediac Bridge (Figure 1). Shediac Bay is an embayment of the Northumberland Strait, a narrow water body between the coast of eastern New Brunswick and Prince Edward Island. The Shediac Bay watershed area covers about 420 km<sup>2</sup> of land area and stretches along approximately 36 km of coastline, from Caissie Cape to Cape Bimet, in south-eastern New Brunswick.

\* Corresponding author



Figure 1. Location of the eelgrass sites in Shediac Bay, New Brunswick, Canada

With a length of about 63 km, Shediac River is an important tributary of the Shediac Bay. The name Shediac is derived from the Micmac name *Esedeik*, meaning "that goes back far", possibly by reference to the configuration of the Shediac Bay or the portage from the Shediac River to the Petitcodiac River (Rayburn, 1975: 252). According to Rémi Donelle (personal communication, 2019), manager of the Shediac Bay Watershed Association, the tide from the Shediac Bay goes far enough inland to provide a deep channel that allows small boats to navigate a certain distance on the river, from the Shediac Bay and the Northumberland Strait.

**2.1.2 Image acquisition:** The UAV images were acquired with a *DJI FC350* camera mounted on a fixed-wing UAV developed by A&L Labs. Canada Inc. (London, Ontario, Canada). Both the camera and UAV were connected to mission planner software to fly at 70 m above the ground with a 70 % overlap between adjacent images. Each image has a spatial resolution close to 5 cm.

Table 1 summarizes the number of images collected at each site, together with the corresponding tide and wind conditions during image acquisition. The images were taken on August 31<sup>st</sup>, 2018, when the eelgrass was fully developed. According to the weather records of the Bouctouche CDA climatological station (Latitude: 46° 25' 49" N; Longitude: 64° 46' 05" W), the air temperature was between 18,3°C and 19,9°C and the relative humidity was between 59% and 63% during the image acquisition.

Site #	Time (AST)	Tide height (m)	Wind speed (km/h)	Wind orientation	Number of images
1	9:48	0.93	13	NNW	143
2	10:09	0.96	13	NW	148
3	10:42	0.99	13	N	133
4	10:59	0.99	11	N	96
5	11:15	1.03	11	N	147

Table 2. The number of images acquired and related environmental conditions in the northern part of the Shediac Bay on August 31, 2018, as a function of the site.

**2.1.3 Field data:** GPS points of the eelgrass beds were collected by Rémi Donelle and his team with a Garmin GPSMap 78s®. GPS data were downloaded and converted to polygons. The GPS data was used to extract spectral values of the following classes: eelgrass, sand floor, deep water, and mud floor, to help to delineate the corresponding training areas. Because the GPS accuracy (about 3 m) is lower than the UAV image spatial resolution (5 cm), the spectral values were extracted from a

11\*11 pixel window and the training areas have a sufficient number of pixels to well represent the classes that were homogenous over a large area

## 2.2 Image processing

For each site, the individual images corresponding to the same band were first mosaicked together with the Pix4Dmapper® software (Pix4D Team, 2019) to produce one mosaic per band. The template used for the mosaicking was *AgRGB* under the advanced category in the processing options. Different settings were attempted to create the best mosaic, and the final processing options used were as follows. For the initial processing, the keypoints image scale, which defines the image size from which the points are extracted compared to the size of the image, was set to the original image size. For the point cloud and mesh, the point cloud densification was set to half, which indicates that half-size images were used to compute additional points. The point density was set to optimal, which set the density of the point cloud. Since the image scale is set to half, one point is computed for every 8 pixels of the initial image. For the DSM, the Orthomosaic, and the Index settings, the box for Google Maps™ tiles and KML was selected to produce a file suitable for Google Maps™. The Pix4Dmapper® software was also used to create one RGB mosaic that incorporates images from all five sites, as shown in Figure 2.

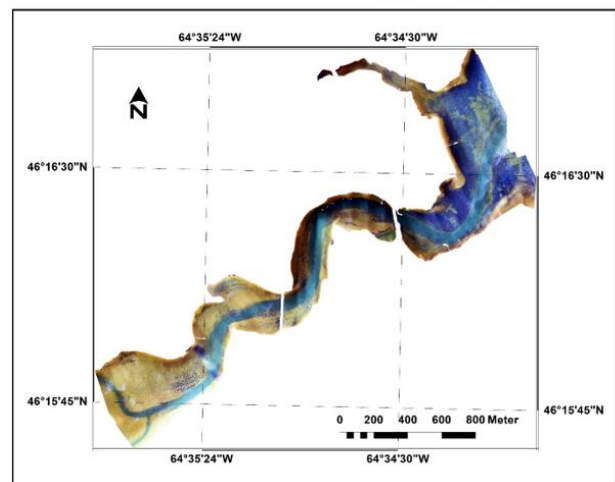


Figure 2. RGB composite for the mosaic created using *Pix4D* with the images acquired over Shediac Bay on August 31st, 2018.

Images were also mosaicked using the PCI Geomatica® software (PCI Geomatics, 2018), after orthorectifying the images individually, using the Pix4D RGB mosaic as reference. After testing various settings, the most effective setting was to use the adaptive filter having the following parameters: filter size (% image) of 20.0 under normalization setting. The colour balance was set to the *bundle* method, and the cutlines were set to *min square difference* with a blending width of 5. The resulting RGB mosaic is showed in Figure 3.

Further analysis was performed for both the Pix4Dmapper® and PCI Geomatica® RGB mosaics. Both mosaic types have a spatial resolution of 5 cm. First, image samples over five areas for each of the four classes (eelgrass bed, deep water channel, sand floor, and mud floor) were taken, and the related extracted digital numbers (DNs) were visually analyzed using bar graphs. The classes appeared to be distinct enough, and training areas of representative areas of each class (eelgrass, sand, deep water, and unknown dark areas) were then delineated. The spectral

signatures were then computed for each class using the three bands, and the corresponding spectral separability was computed by the Jefferies-Matusita (J-M) distance. The closer the J-M distance to 2, the better the spectral separability between two classes.

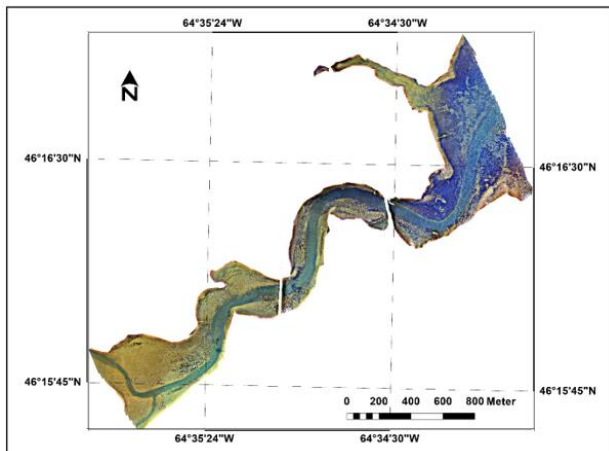


Figure 3. RGB composite for the mosaic created using PCI Geomatica with the images acquired over Shediac Bay on August 31st, 2018.

The training areas were then used into a Maximum likelihood classifier (MLC) using the *MLC* program of PCI Geomatica® (PCI Geomatics, 2018) that was applied to the three bands. The MLC is a parametric supervised classifier that assumes a Gaussian distribution of grey level values for each class and the same probability of occurrence for each class in the image. It classifies each pixel  $x$  in class  $i$  by maximizing the following discriminant function (Strahler, 1980):

$$g_i(x) = \ln(p(i)) - \frac{1}{2}(X - M_i)^t \Sigma_i^{-1}(X - M_i) - \frac{1}{2} \ln|\Sigma_i| - \frac{k}{2} \ln(2\pi) \quad (1)$$

where  $g_i(x)$  = discriminant function for class  $i$  and pixel  $x$   
 $p(i)$  = a priori probability for class  $i$   
 $X$  = grey level value of pixel  $x$  in each input image  
 $M_i$  = mean vector for class  $i$   
 $\Sigma_i$  = covariance matrix for any class  
 $|\Sigma_i|$  = determinant of the covariance matrix  $\Sigma_i$   
 $\Sigma_i^{-1}$  = inverse of the covariance matrix  $\Sigma_i$   
 $(X - M_i)^t$  = transposed matrix of  $(X - M_i)$   
 $k$  = number of input images used in the classification

The classification accuracy was assessed using the confusion matrix and the related class User's and Producer's accuracies, average accuracy, overall accuracy, and Kappa coefficient. The average accuracy is the simple average of the class accuracies, whereas the size of the class in the image weights the overall accuracy. The Kappa coefficient is a weighted measure of agreement of the number of correctly classified pixels: the closer to one, the more accurate the classification.

### 3. RESULTS

#### 3.1 Pix4D RGB mosaic

**3.1.1 Spectral separability:** The potential separability of the four classes (eelgrass, deep water, sand floor, and mud floor) in the Pix4D® RGB mosaic was first assessed through a graphical comparison of the DN values of the four classes at each of the five selected areas of each class. Graphs were produced for channel 1 or blue band (Figure 4), channel 2 or green band (Figure 5), and channel 3 or red band (Figure 6). The four classes are separated in the blue band (Figure 4) for which the eelgrass has distinct DN values. This is not true for the green (Figure 5) and red bands (Figure 6). This is because the blue band radiation penetrates the water better than the other band radiation, therefore allowing better discrimination amongst the classes.

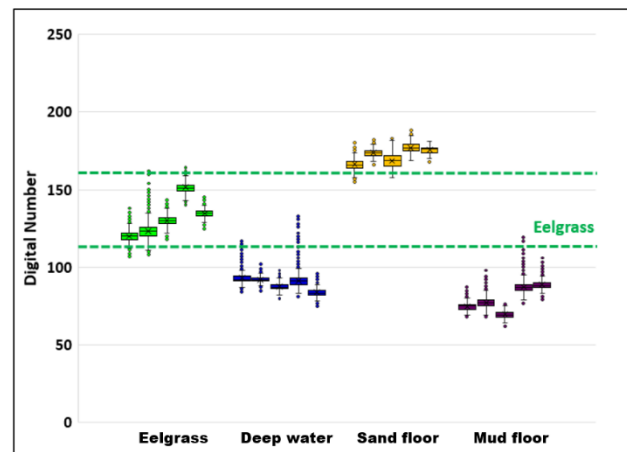


Figure 4: Channel 1 (blue band) comparison of the DN values for the four classes in the Pix4D RGB mosaic of Shediac Bay. The green dashes indicate the range of DN values that correspond to eelgrass.

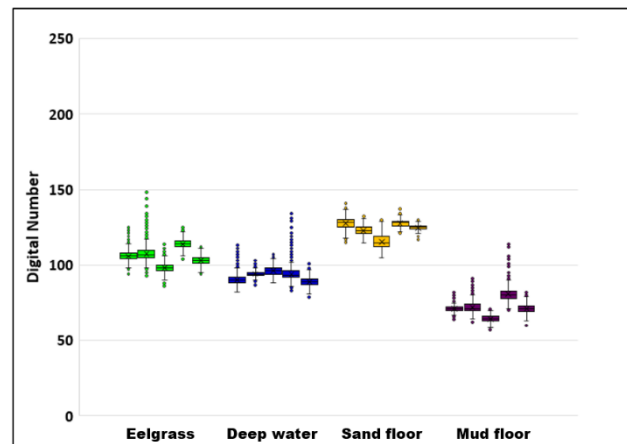


Figure 5: Channel 2 (green band) comparison of the DN values for the four classes in the Pix4D RGB mosaic of Shediac Bay.

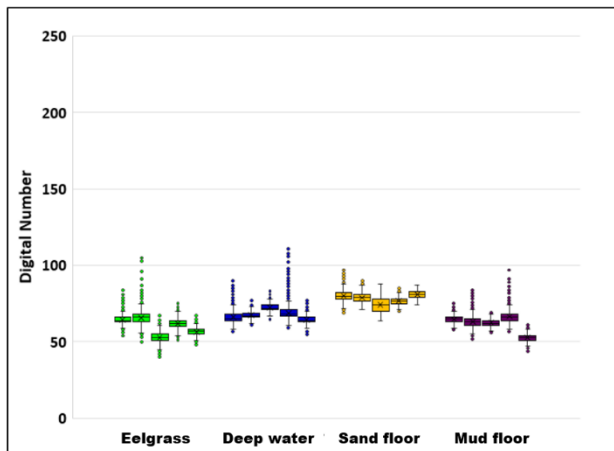


Figure 6: Channel 3 (red band) comparison of the DN values for the four classes in the Pix4D RGB mosaic of Shediac Bay.

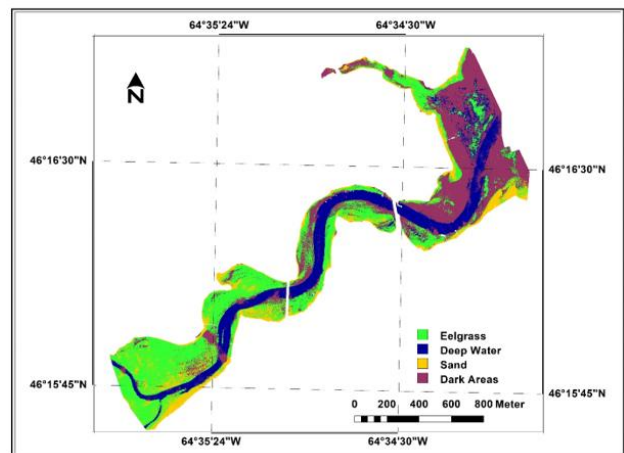


Figure 7. Classified image produced with the Maximum Likelihood Classifier (MLC) applied to the Pix4D® RGB mosaic of Shediac Bay.

Training areas were then delineated for each class of the Pix4D® RGB mosaic, and their related spectral signatures were then used to assess the class spectral separability using the J-M distance (Table 2). This table shows that the spectral separability between *Eelgrass* and *Mud floor* is excellent (above 1,9), and the spectral separability between the *Eelgrass* class and the *Deep water* or *Sand floor* classes is slightly lower, but near as good (above 1,8).

Name	Deep Water	Sand floor	Mud floor
Sand floor	1,999	-	-
Mud floor	1,698	1,999	-
Eelgrass	1,883	1,845	1,955

Table 2. J-M distance computed with the class training areas delineated from the Pix4D RGB mosaic of Shediac Bay, for each class (eelgrass, deep water, sand, and unknown dark areas).

**3.1.2 Classification:** The Pix4D® RGB mosaic was then classified using the MLC, and the related confusion matrix is presented in Table 3. The classification accuracy is high, with a very high average accuracy (98,33%) overall accuracy (98,17%) and Kappa coefficient (0,975). The related classified image is shown in Figure 7.

Name	Deep water	Sand floor	Mud floor	Eelgrass	User's accuracy
Deep water	97,46	0,00	2,29	0,24	97,46
Sand floor	0,00	99,93	0,00	0,07	99,93
Mud floor	2,14	0,00	97,68	0,18	97,68
Eelgrass	0,12	1,45	0,18	98,25	

Table 3. Confusion matrix (in %) computed for the MLC classified image produced from the Pix4D RGB mosaic of Shediac Bay.

### 3.2 PCI Geomatica RGB mosaic

**3.2.1 Spectral separability:** The potential for separability of the four classes in the PCI Geomatica RGB mosaic was assessed through a graphical comparison of the DN values of the four classes at each of the five selected areas of each class. Graphs were produced for channel 1 or blue band (Figure 8), channel 2 or green band (Figure 9), and channel 3 or red band (Figure 10).

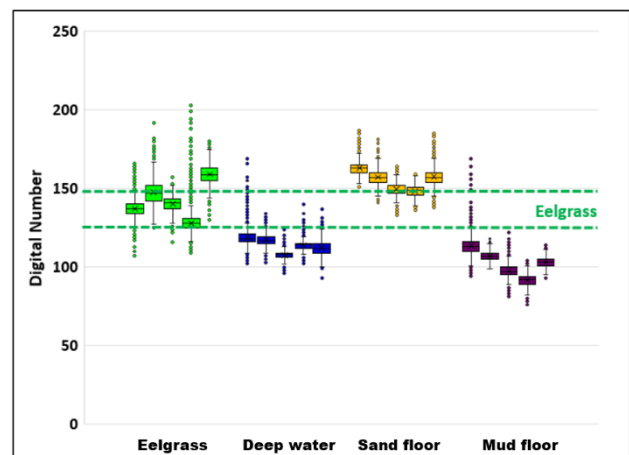


Figure 8: Channel 1 (blue band) comparison of the DN values for the four classes in the PCI Geomatica RGB mosaic of Shediac Bay. The green dashes indicate the range of DN values that correspond to eelgrass.

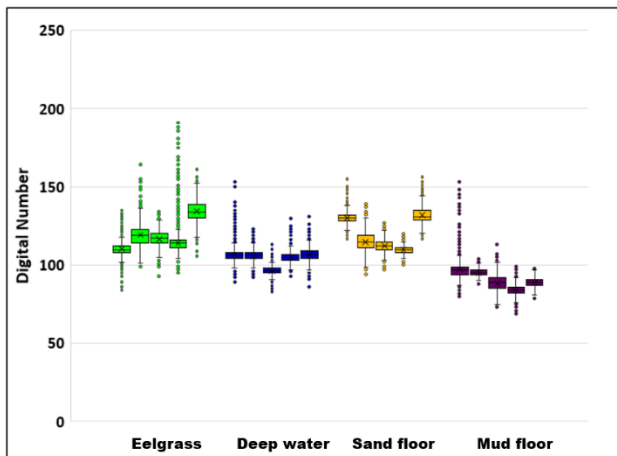


Figure 9: Channel 2 (green band) comparison of the DN values for the four classes in the PCI Geomatica RGB mosaic of Shediac Bay.

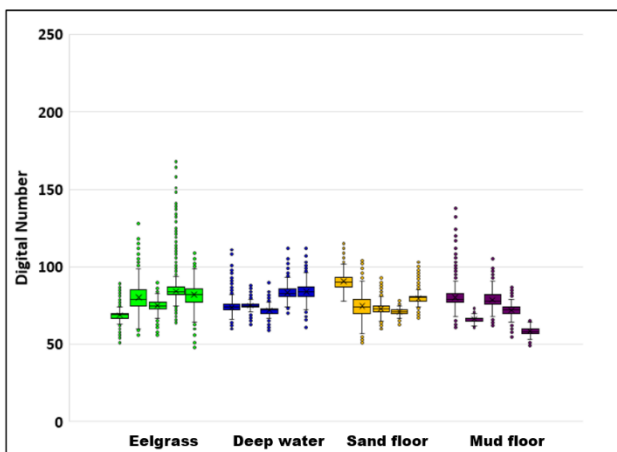


Figure 10: Channel 3 (red band) comparison of the DN values for the four classes in the PCI Geomatica RGB mosaic of Shediac Bay.

The four classes are almost clearly separated in the blue band (Figure 8), and the eelgrass has distinct DN values, with only some values overlapping with the sand floor class. This is not true for the green and red bands (Figures 9 and 10). This is because the blue band radiation penetrates the water better than the other band radiation, therefore allowing better discrimination amongst the classes.

Training areas were then delineated for each class of the PCI Geomatica RGB mosaic, and their related spectral signatures were used to assess the class separability using the J-M distance. Table 4 shows that the spectral separability between eelgrass and the dark areas is almost good (above 1,9) and the spectral separability between the eelgrass and the deep water or sand is quite poor

Name	Deep water	Sand floor	Mud floor
Sand floor	1,999	-	-
Mud floor	1,458	1,996	-
Eelgrass	1,144	1,645	1,856

Table 4. J-M distances computed with the class training areas delineated from the PCI Geomatica RGB mosaic of Shediac Bay for each class (eelgrass, deep water, sand, and unknown dark areas).

**3.2.2 Classified image:** The PCI Geomatica RGB mosaic was then classified using the MLC, and the related confusion matrix is presented in Table 5. The classification accuracy is relatively good, with an average accuracy at 89,47%, an overall accuracy of 87,91%, and a kappa coefficient of 0.83428. However, the accuracy is the lowest for the eelgrass class, mainly because of a confusion with the sand and deep-water classes (Table 5). The related classified image is shown in Figure 11.

Name	Deep water	Sand floor	Mud floor	Eelgrass	User's accuracy
Deep water	87,41	0,00	6,37	6,22	87,41
Sand floor	0,00	97,91	0,00	2,09	97,91
Mud floor	6,10	0,00	92,88	1,02	92,88
Eelgrass	12,14	8,01	0,18	79,67	79,67
Producer's accuracy	82,74	92,44	93,41	89,52	

Table 5. Confusion matrix (in %) computed from the MLC classified image produced from the PCI Geomatica RGB mosaic of Shediac Bay.

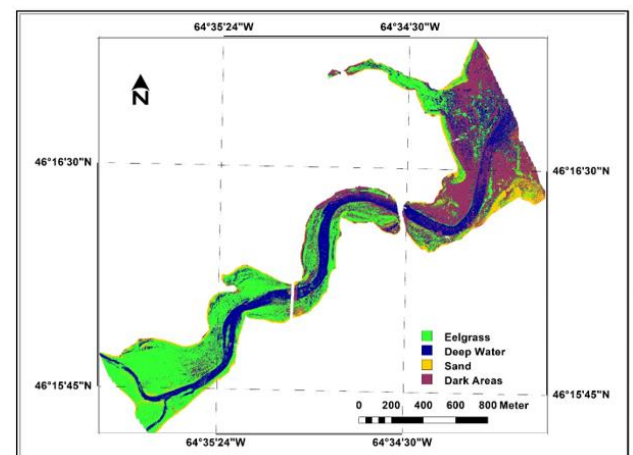


Figure 11. Classified image produced with the *Maximum Likelihood Classifier* (MLC) applied to the PCI Geomatica RGB mosaic of Shediac Bay.

#### 4. DISCUSSIONS AND CONCLUSIONS

Our study indicates that the Pix4D mosaicking is superior to the PCI Geomatica mosaicking when the MLC classifier is applied to an RGB mosaic for mapping eelgrass beds. The Pix4D RGB mosaic has more spectrally separable classes (Table 2), resulting in high classification accuracies (Table 3). The PCI Geomatica RGB mosaic had lower separability for the four classes (Table 4), resulting in lower classification accuracy (Table 5). Although our study shows that mapping eelgrass beds with UAV RGB mosaics is possible, some techniques of image acquisition can be improved to create a better mosaic, which will lead to a more accurate classification.

One problem that arose during the process was the difference in sun illumination over the image. The images over the five eelgrass sites were acquired at different times of the day, leading to differences across the RGB mosaic. In future work, the images could be taken in overcast weather as this will reduce the problem of the difference in sun illumination over the image. This would also eliminate the problem of cloud shadows seen in the image, which is evident in both RGB mosaics. Also, capturing the images in overcast may reduce sun glint seen in both RGB mosaics. If glint still occurs, some methods remove glint from

images. However, most of them use the NIR image (Kay et al., 2009), and they cannot be applied to our images that were only acquired in the RGB bands. Future work should also incorporate a bathymetric map in the classification process. This would create more accurate results as it provides another level of information for the classification process.

It is also important to note that the Pix4Dmapper® program works best for coastal images with land present in the image. Problems with mosaicking arise when the image is acquired entirely over water. This is because the program has difficulties in creating a densified point cloud when the features on the imagery are homogenous, such as water or dense forests. This is a documented problem with the program, and the company suggests a few solutions by adjusting the settings. In this study, the suggestions were used to create the best possible mosaics. If this solution does not work, it is recommended to take new images that include land. For this reason, this software is better suited for mosaicking eelgrass images acquired close to shore, such as in this study, but not for the images acquired out in the bay.

The high classification accuracy obtained with the Pix4D RGB mosaic is encouraging, but it is an assessment of the classified image accuracy that is different than the true mapping accuracy. A more robust and independent accuracy assessment is to compare the resulting classified image with an independent set of GPS field observation data acquired over the validation sites. We will perform such a comparison with an eelgrass map that was created from sonar measurements. The map we produced shows that there is more eelgrass in the river area than in the bay. This may be influenced by the depth of the water or other environmental factors.

This study was beneficial to determine the best way to create an RGB mosaic using UAV images that will be successful in mapping eelgrass. If restoration efforts are made in these areas in the future, the map can be used as a base to compare the restoration progress.

#### ACKNOWLEDGMENTS

The authors would like to thank Eva Dickson from Oceans Management Program at the Department of Fisheries and Oceans Canada (DFO) in Moncton for the sonar maps, Rémi Donelle, manager of the Shediac Bay Watershed Association for the GPS data, and Brian Gaudet who piloted the UAV during image acquisition. The study was funded by Environment and Climate Change Canada - Atlantic Ecosystems Initiative Program, and the New Brunswick Environmental Trust Fund.

#### REFERENCES

Biber, P.D., Harwell, M.A., Cropper, W.P., 2004: Modelling the dynamics of three functional groups of macroalgae in tropical seagrass habitats. *Ecological Modelling*, 175(1), 25-54.

Heck, K.L., Able, K.W., Roman, C.T., Fahay, M.P., 1995: Composition, abundance, biomass, and production of macrofauna in a New England estuary: comparisons among eelgrass meadows and other nursery habitats. *Estuaries*, 18(2), 379-389.

Kay, S., Hedley, J.D., Lavender, S., 2009: Sun glint correction of high and low spatial resolution images of aquatic scenes: a review

of methods for visible and near-infrared wavelengths. *Remote Sensing*, 1, 697-730.

Konar, B., Iken, K., 2017: The use of unmanned aerial vehicle imagery in intertidal monitoring. *Deep Sea Research, Part II: Topical Studies in Oceanography*, 147, 79-86.

Morris, C.J., Gregory, R.S., Laurel, B.J., Methven, D.A., Warren, M.A., 2011: Potential effect of eelgrass (*Zostera marina*) loss on nearshore Newfoundland fish communities, due to invasive green crab (*Carcinus maenas*). DFO Canadian Science Advisory Secretariat Research Document, Fisheries and Oceans Canada, Document 2010/140, 17 pages.

Pajares, H., 2015: Overview and Current Status of Remote Sensing Applications Based on Unmanned Aerial Vehicles (UAVs). *Photogrammetric Engineering & Remote Sensing*, 81(4), 281-329.

Peasgood, S., Valentin, M., 2015: Drones: A Rising Market. An industry to lift your returns. Sophic Capital, Toronto, 11 pages.

PCI Geomatics, 2018. PCI Geomatica® Software, Version 2018, Markham (Ontario).

Pix4D Team, 2029, Pix4Dmapper® Software, Version 4.5.2, Prilly (Switzerland).

Rayburn, A., 1975: Geographical Names of New Brunswick. Ottawa, Surveys and Mapping Branch, Department of Energy, Mines and Resources, 1975, 304 pages.

Short, F.T., Wyllie-Echeverria, S., 1996: Natural and human-induced disturbance of seagrasses. *Environmental Conservation* 23(1), 17-27.

Short, F.T., Davis, R.C., Kopp, B.S., Short, C.A., Burdick, D.M., 2002: Site-selection model for optimal transplantation of eelgrass *Zostera marina* in the northeastern US. *Marine Ecology Progress Series*, 227, 253-267.

Short, F.T., McKenzie, L.J., Coles, R.G., Vidler, K.P., Gaeckle, J. L., 2006: SeagrassNet. Manual for scientific monitoring of seagrass habitat. Worldwide edition, University of New Hampshire Publication, 75 pages.

Ventura, D., Bruno, M., Lasinio, G.J., Belluscio, A., Ardizzone, G., 2016: A low-cost drone based application for identifying and mapping of coastal fish nursery grounds. *Estuarine, Coastal and Shelf Science*, 171, 85-98.

Ward, D.H., Markon, C.J., Douglas, D.C., 1997: Distribution and stability of eelgrass beds at Izembek Lagoon, Alaska. *Aquatic Botany*, 58(3), 229-240.